



Corrosion inhibition of brass in artificial drinking water by mineral compound

M. Nihorimbere^{1*}, Y. Kerroum¹, A. Guenbour¹, M. Kacimi¹,
A. Bellaouchou¹, R. Tour^{2,3}, A. Zarrouk⁴

¹Laboratoire des Matériaux, Nanotechnologies et Environnement, Faculté des Sciences de Rabat, Université Mohammed V-Rabat (Maroc)

²Laboratoire d'Ingénierie des Matériaux et d'Environnement : Modélisation et Application, Faculté des Sciences, Université Ibn Tofail, BP 133, Kénitra 14 000, Morocco.

³Centre Régional des Métiers de l'Éducation et de la Formation (CRMEF), Avenue Allal Al Fassi, Madinat Al Irfane BP 6210 Rabat, Morocco.

⁴LC2AME, Faculty of Science, First Mohammed University, PO Box 717, 60 000 Oujda, Morocco.

Received 21 Jun 2016, Revised 23 Sept 2016, Accepted 28 Sept 2016

*For correspondence: Email: nihomana@yahoo.fr tel : +212 6 8070 5962

Abstract

The corrosion behavior of brass in Simulated Drinking Water (SDW) without and with mineral compound (P) has been investigated using potentiodynamic polarization, electrochemical impedance spectroscopy (EIS) and optical microscope. The obtained results showed that the inhibitor addition significantly reduced the corrosion current density. The inhibition efficiency increased with concentration of inhibitor to reach a maximum of 84 % at 1000 ppm. Polarization studies showed that this inhibitor acted as cathodic type for brass in Simulated Drinking Water (SDW). The Appropriate electric equivalent circuit model was used to calculate the impedance parameters. The corrosion parameters obtained from polarization curves and from EIS spectra are in good concordance and point out the inhibitory action of mineral compound (P). Optical microscope observation after three days of immersion showed the formation of mixed products with inhibitor.

Keywords: Brass, Simulated drinking water, Corrosion inhibition, Electrochemical measurement, Optical microscope.

1. Introduction

Copper and its alloys are used in marine environments, heat exchanger tubes in absorption refrigeration systems, and water distribution systems due to their excellent electrical and thermal conductivity, good machineability, corrosion resistance, and low cost [1-3]. They have become the material of choice in the deposition of highly conductive interconnects on an integrated circuit. Brass is widely used as tubing material for condensers in cooling water systems. The majority of the marine propellers are made from copper and its alloys. Although copper and its alloys are resistant toward the influence of atmosphere and many chemicals, they are susceptible to corrosion problems such as dezincification and pitting corrosion in aggressive media.

Brass is susceptible to a corrosion process known as dezincification and this tendency increases with increasing zinc content of the brass [4,5]. During the past decade, many techniques have been used to minimize the dezincification and corrosion of brasses. One of the techniques for minimizing corrosion is the use of inhibitors. The effectiveness of the inhibitor varies with its concentration, the corrosive medium and the surface properties of the alloy. Many inhibitors have been used to minimize the corrosion of brass in different media [6-11].

Due to these problems, organic inhibitors are being replaced by less toxic inorganic ones. The usually inorganic inhibitors investigated for copper alloys are chromate CrO_4^{2-} , molybdate MoO_4^{2-} , tetraborate $B_4O_7^{2-}$ and Tungstate WO_4^{2-} [12,13]. Chromate is considered as efficient corrosion inhibitor due to a formation of an oxide film on the metal surface which passivate the electrode surface, but it is also known that it can promote corrosion acting as a cathodic reactive. However, the main drawback is the toxicity of chromate anion. The logical alternative to hexavalent chromium is the molybdate and tetraborate species. Nevertheless, molybdate and tetraborate showed very low inhibition effect. Also, it is not feasible to use tungstate alone as a corrosion

inhibitor due to its low oxidizing ability and high cost. Inhibitor efficiencies for these species are: 1.56% for molybdate, 51% for tetraborate and 78.6% for chromate [12].

The corrosion inhibition of copper and its alloys used in installations such as power generation and sea water desalination becomes an important challenge. The inhibitory action of organic and inorganic compounds, which are generally used are well known and widely described in the literature. It was found that most of them present the disadvantage of high degree of toxicity and are dangerous to humans and the environment [14].

It is now required to design new environment-friendly inhibitors. Recent researches have been oriented towards the use of corrosion inhibitors called "green" very effective, low-cost, non-toxic and biodegradable [15]. In this regard, studies have been made on the use of rare earths as corrosion inhibitors for various types of metals and alloys, such as aluminum, [16,17] zinc, [18,19] bronze, [20] steel [21] and manganese, [22,23] but rarely for Brass.

In this study, mineral compound was tested as green inhibitor on brass in artificial drinking water using electrochemical tests, such as potentiodynamic polarization and impedance spectroscopy. The morphology of the brass surface was examined by optical microscope.

2. Materials and methods

2.1. Sample and preparation

The metal sample used in this study was brass (from National Drinking Water Office) used as tap water. The working electrode used having the chemical composition as wt (%) 56.24 Cu, 40.494 Zn, 2.345 Pb, 0.224 Fe, 0.2135 Sn, 0.114 Ni, 0.051 Al, 0.008 Mn, 0.003 As, and 0.0013 Si. This electrode was embedded in epoxy resin, leaving a geometrical surface area of 0.78 cm² exposed to the electrolyte. Prior to the measurements, the exposed surface was pre-treated by using decreased emery papers grade (240, 400, 600, 1000, and 1200) and then rinsed by double distilled water.

2.2. Electrolyte

The experiments were carried out using Simulated Drinking Water (SDW) simulating the average composition of the drinking water. The mineral base composition was (735 mg/L CaCl₂·2H₂O, 493 mg/L MgSO₄, 658 mg/L NaCl, 168 mg/L NaHCO₃) already used by other researcher [24]. Electrolyte pH was fixed at 7.6 ± 0.2 by titration 0.1 M HCl.

It is accepted that high chloride, low hardness and low alkalinity waters are especially prone to dezincification, justifying the choice of this water [25]. All the experiments were carried out at room temperature (295 ± 2 K).

2.3. Mineral compound characterization

Our study was focused to study the inhibition of mineral compound (P) as green inhibitor on brass in simulated drinking water which composition indicated type Aragonite (Figure 1). Aragonite is the metastable form calcium carbonate mainly component of pearl, coral, and shells living in many things. The color is grey and collected near the border of the sea. The aragonite crystallizes in the orthorhombic form. This inhibitor would be harmless of human health and friendly with the environment.

2.4. Electrochemical measurements

The electrochemical measurements were carried out using a potentiostat/galvanostat (Volta lab PGZ301). A three-electrode electrochemical cell and instrumentation employed are standard and have been reported before [26, 27]. A saturated calomel electrode ((SCE) E=0.24 V/SHE). A Luggin capillary minimized the Ohmic drop. A Pt wire was used as counter electrode. Brass electrodes were pre-reduced in the corresponding electrolyte at -1.15 V/SCE for 5 min to begin with a reproducible surface. Then, the electrodes were kept at the corrosion potential (E_{corr}) for 1 h. The passive layer was stable and the open circuit potential remained constant.

The potentiodynamic current-potential curves were recorded by changing the electrode potential automatically from -1.1 to 0.5 V/SCE with scan rate of 1 mV s⁻¹. Electrochemical impedance spectroscopy (EIS) tests were performed at E_{corr}. The response of the electrochemical system to ac excitation with a frequency ranging from 20 KHz to 5 mHz and peak to peak amplitude of 10 mV was measured with data density of 10 points per decade. The impedance data were analyzed and fitted with the simulation Z-View 2.80, equivalent circuit software. All the measurements were carried out in air saturated solutions and at ambient temperature (295 ± 2 K). Each experiment was performed in a freshly prepared solution and with a newly ground electrode surface. The experiments were repeated to ensure reproducibility.

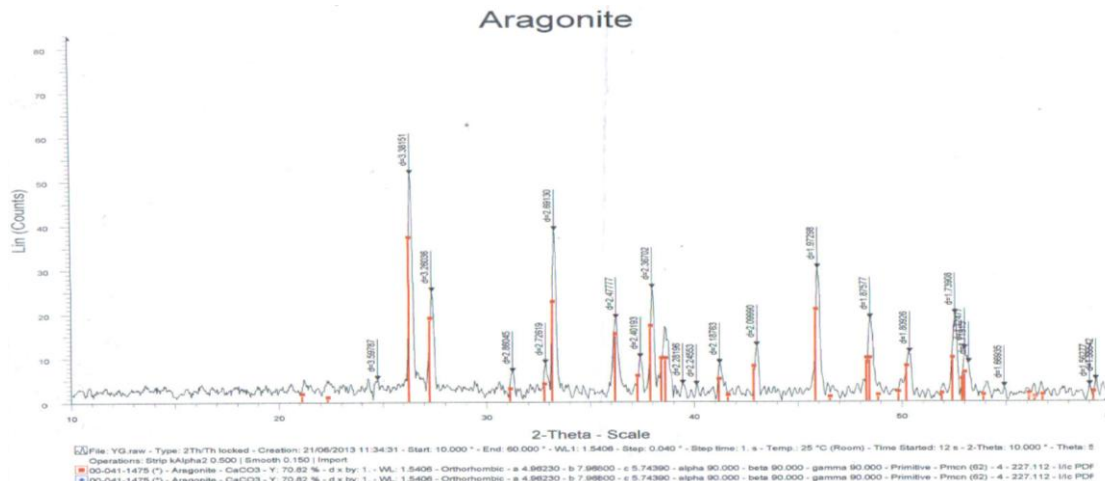


Figure 1: XRD pattern of the aragonite from the border of sea in Morocco.

2.5. Optical microscopy observations

The optical microscopy observations of metal surface (micrograph) were performed with an optical microscope Leica CTR 6000 (Optical microscope type DFC 295) allowing for magnifications of 50 to 1000 times. A digital sensor mounted on the microscope used to view the different microstructures of our parts. The acquisition of the pictures is made by computer with appropriate software. Images are taken after 30 days of immersion in the presence and absence of inhibitor.

3. Results and discussion

3.1. Potentiodynamic Polarization Studies

3.1.1. Effect of concentration

The effect of mineral compound (P) on the anodic and cathodic polarization behavior of brass in simulated drinking water at 295 K are shown in Figure 2. Their corresponding kinetic parameters including corrosion current density (i_{corr}), corrosion potential (E_{corr}) and anodic and cathodic Tafel slopes (b_a and b_c), are given in Table 1. The i_{corr} values were used to calculate the inhibition efficiency, $\eta_{Tafel}(\%)$, using the following equation:

$$\eta_{Tafel}(\%) = \frac{i_{corr}^0 - i_{corr}}{i_{corr}^0} \times 100 \quad (1)$$

where i_{corr}^0 and i_{corr} are the corrosion current densities for brass electrode in the uninhibited and inhibited solutions, respectively.

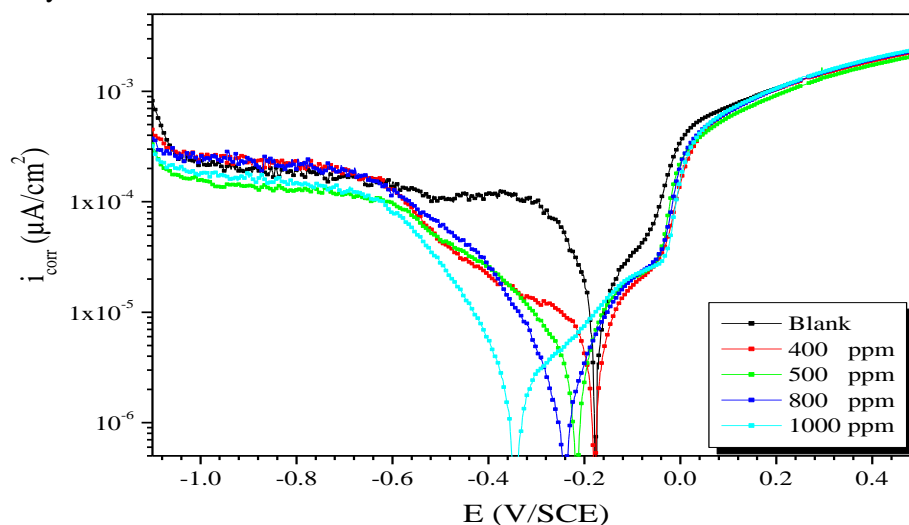


Figure 2: Potentiodynamic polarization curves for brass in simulated drinking water containing different concentrations of inhibitor (P) at 295 K.

In Figure 2, both anodic and cathodic reactions of brass electrode were inhibited after addition of inhibitor to simulated drinking water, and its inhibition became more pronounced with increasing its concentration. This result indicated that the addition of P reduced brass anodic dissolution and also retards the oxygen reduction. In addition, it is noted that the P addition shifted the corrosion potential towards the negative direction in comparison to the uninhibited solution. This phenomenon may be attributed to the change of adsorption behavior of P on the metallic surface with its concentration [28]. In the anodic branch, the action of P on the anodic behavior of brass is independent of the electrode potentials and leads to passivation pseudo-plate due a deposit film on the brass surface [8]. This trend increased with increasing the inhibitor concentration. It is believed that the decrease of the anodic dissolution process is attributed to the precipitation of insoluble complexes on the electrode surface [26,27]. It has also been known that the inhibitor molecules were able to induce some corrosion activity of brass during the initial anodic process; probably due to the inhibitor molecules displace some hydrated layers of brass/hydroxyde film in order to create more favorable sites for the formation stable protective layer [29].

However, Figure 2 revealed that the P addition in the corrosive solution decreased the cathodic current densities, and no significant change was detected in the appearance of the cathodic curves indicating that the cathodic process was unchanged. This indicated the adsorption of P molecules on the brass surface and the retardation of corrosion without altering the cathodic reaction mechanism by merely blocking the active sites [30]. In the cathodic range, dissolved oxygen in the solution takes over the cathodic reaction of brass in SDW media as shown in the following Eq. (2)



Further inspection of Table 1 revealed that the anodic Tafel slope values (b_a) remain almost unchanged upon increasing of P concentration, indicating that the anodic reaction mechanism is not changed by P addition. It is observed that the inhibition efficiency increased with increasing of P concentration to reach a maximum value of 84 % at 1000 ppm of P.

Table 1: Data obtained from the potentiodynamic polarization curves of brass in SDW-solution in the absence and presence of various concentrations of mineral compound (P).

	Conc. (ppm)	$-E_{corr}$ (mV/SCE)	i_{corr} ($\mu A/cm^2$)	b_c (mV/dec)	b_a (mV/dec)	η_{Tafel} (%)
Blank	00	175.5	5.7	87.2	122.1	—
	400	176.6	2.5	89.6	130.8	56
P	500	209.3	1.6	133.6	68.1	70
	800	244.8	1.2	116.0	116.7	78
	1000	337.9	0.9	93.0	102.0	84

In literature, it has been reported that an inhibitor can be classified as an anodic-or cathodic-type when the change in E_{corr} (Blank) value is larger than 85 mV/SCE [31,32] and as mixed type if displacement in E_{corr} is less than 85 mV. In comparison with the brass in the blank, the E_{corr} values move largely in the negative direction and the displacements (162.4 mV/SCE) are more than 85 mV/SCE, which indicates that mineral compound P could be classified as a cathodic-type inhibitor and this mineral has the advantage of being non-toxic and readily available. It was obvious that current density decreased with increasing concentration of mineral compound (5.7 $\mu A/cm^2$ for blank to 0.90 $\mu A/cm^2$). It is well known that brass may undergo a non-uniform corrosion as the pitting corrosion in drinking water due high pH, high free chlorine residual and low alkalinity. This observation can be seen in the anodic potential up 200 mV/SCE.

3.2. Electrochemical impedance spectroscopy

Nyquist plots of brass in SDW-solution and in the presence of various concentrations of P and at 295 K are given in Figure 3. As seen in Figure 3, the Nyquist diagrams of brass have two capacitive contributions represented by two semi-circles for all concentrations except blank solution. The capacitive loop appearing at higher frequency range was attributed to charge transfer resistance of the corrosion process and diffusion layer resistance of metal/solution boundary phase [33,34]. The capacitive loop shown at low frequency is related to film resistance caused by the formation of the inhibitor layer [35,36].

The slightly depressed nature of the semi-circles in Nyquist diagrams is characteristic for the solid electrode which has the center below the x-axis. Impedance spectroscopy studies on the double layer capacitance at solid electrodes usually show deviations from ideal behavior. The dispersion has been attributed to roughness and other inhomogeneity of the solid electrode and also anion adsorption. The anomalous capacitance dispersion can be represented by a so-called constant phase element, CPE [37], and the impedance of the CPE (Z_{CPE}) can be expressed as follows [38,39]:

$$Z_{CPE} = \frac{1}{Y_0 (j\omega)^n} \quad (3)$$

where Y_0 is the CPE constant, n is the CPE exponent. j is the square root of -1, and ω is the angular frequency. Depending on the value of n , CPE can represent a resistance. n is a measure of non-ideality of the capacitor and has a value ranging from -1 to 1 [40].

EIS measurements demonstrated that the diameters of capacitive loops were increased with increasing of P concentration which indicated an increase in the polarization resistance of brass corrosion. The increase in resistance of Nyquist diagrams proved an increase in surface coverage. This can be seen distinctly from Figure 3. The adsorbed inhibitor molecules formed a protective film via insulating [41], the brass surface from solution and making the corrosion reaction more difficult.

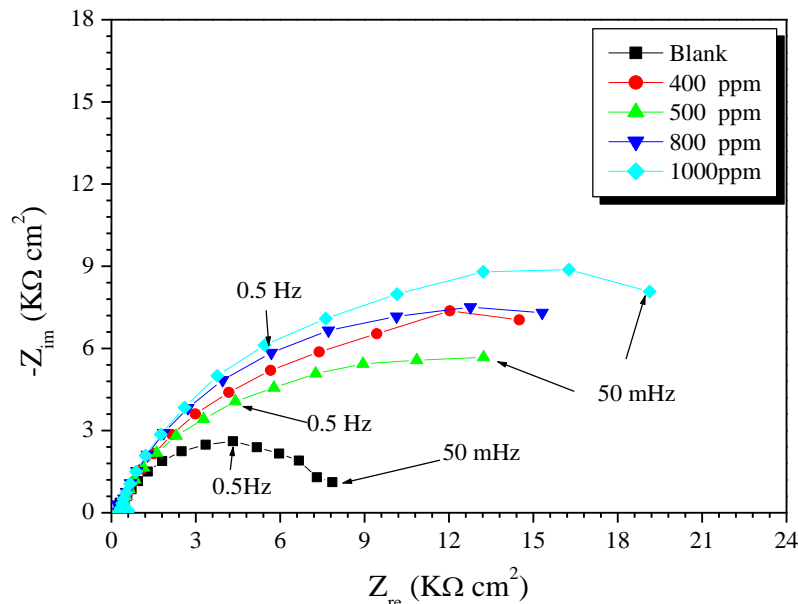


Figure 3: Nyquist diagrams of brass in SDW-solution and in the presence of various concentrations of P.

The physical description of the corrosion process of brass in the studied medium was analyzed by modeling the metal/solution interface to an equivalent electrical circuit. The EIS data were fitted to the most probable equivalent circuit for modeling metal/solution interface; therefore two types of equivalent circuits were proposed (Figure 4).

In Figure 4a an equivalent circuit with one semicircle was used for describing the inhibitor free brass/solution interface at 295 K. The elements of the circuit can be named as; R_s is the solution resistance, R_{ct} is the charge transfer resistance, R_d is the diffuse layer resistance which is related to the transportation resistance of ions from metal surface to solution or vice versa [42] and CPE_{dl} is the constant phase element of the double layer. The semicircle can be described as an overlapping of the double layer resistance (R_{ct}) and the diffuse layer resistance (R_d) in the brass/solution system which are not possible to distinguish between. Therefore the polarization resistance (R_p) can be calculated by summing these two resistances ($R_p = R_{ct} + R_d$).

The equivalent circuit shown in Figure 4b was used for fitting electrochemical responses of brass which have two loops in the Nyquist plots. As shown in Figure 4b two different elements were added into the circuit in order to define the brass/solution interface accurately. These added circuit elements were presented as R_f and R_{ox} . R_f reflects the film resistance of adsorbed inhibitor molecules, R_{ox} is the oxide film resistance that formed

on brass surface, CPE_f is the constant phase element of the film layers and CPE_{dl} is the constant phase element of the double layer in the equivalent circuit.

The second loop that can be observed in the Nyquist diagrams of inhibitor free solutions was related with the oxide layer on brass formed in SDW-solution. In these cases there were no inhibitor molecules in the solution, so the film resistance R_f should not take part in the polarization resistance expression. The total resistance may be stated as $R_p = R_{ct} + R_d + R_{ox}$ and CPE_f was related to the oxide film of brass.

In the case of P containing solutions, the Nyquist diagrams were described with the equivalent circuit shown in Figure 4b. In these diagrams there were two loops which were related to the faradaic process and film formation. The faradaic process was associated with the high frequency part of the impedance diagrams and represented with R_{ct} , R_d and CPE_{dl} elements similar to the model mentioned in Figure 4a. The second loop which was observed in the lower frequency region was attributed to resistance of both the oxide film of brass and the adsorption of P. The total polarization resistance can be summed up as $R_p = R_{ct} + R_d + R_{ox} + R_f$ and CPE_f was the capacitance of both oxide and complex film layer.

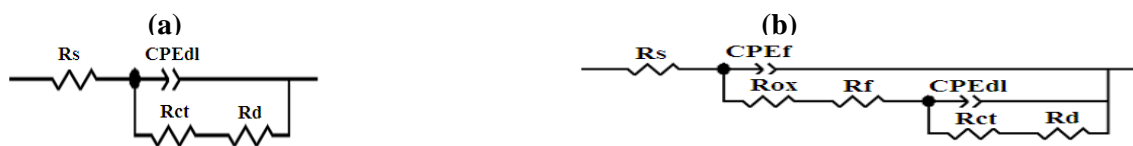


Figure 4: Proposed equivalent circuits for impedance analysis and interpretation of brass-SDW solution system. Equivalent circuit for having (a) one semi circle (b) two semicircles in impedance spectra.

The data obtained by fitting the EIS results were summarized in Table 2. It is noted that the R_p values increased significantly with the concentration of P whereas the CPE_f values decreased. This suggests that the surface film formed in the presence of P was thicker, less permeable and strongly adsorbed [43]. The inhibition efficiencies were calculated at different concentrations utilizing the polarization resistance values according to the following equation.

$$\eta_{EIS} (\%) = \frac{R_{p(inh)} - R_p}{R_{p(inh)}} \times 100 \quad (4)$$

where $R_{p(inh)}$ and R_p are polarization resistance values with and without P, respectively

Table 2: Impedance parameters for brass corrosion in SDW-solution at different concentration of P.

	Conc. (ppm)	R_s ($\Omega \text{ cm}^2$)	CPE_{dl}		$R_{ct}+R_d$ ($\Omega \text{ cm}^2$)	CPE_f		R_f ($\Omega \text{ cm}^2$)	R_p ($\Omega \text{ cm}^2$)	η_{EIS} (%)
			$Y_0 \times 10^4$ ($S^n \Omega \text{ cm}^{-2}$)	n		$Y_0 \times 10^4$ ($S^n \Omega \text{ cm}^{-2}$)	n			
Blank	00	277.5	1.7041	0.779	6501	—	—	—	6501	—
P	400	290.9	1.2916	0.608	10538	0.3286	0.838	4664	15202	57.2
	500	319.9	0.9018	0.735	11864	0.3349	0.814	10455	22319	70.9
	800	280.7	0.6859	0.531	13969	0.4625	0.871	12683	26652	75.6
	1000	279.5	0.4829	0.691	17999	0.4998	0.821	16989	34988	81.4

It is also apparent from Table 2 that the values of CPE_{dl} decreased with increasing P concentration. This decrease in CPE_{dl} values suggested a decrease in the dielectric constant and/or an increase in the double layer thickness. This can be explained as a result of adsorption of P molecules onto the brass surface which have lesser dielectric constant compared with desorbed water molecules. Thus, the brass surface was protected against the corrosive medium [44, 45].

3.3. Optical micrograph results

Figure 5 shows images took by optic microscopy without and with 1000 ppm of P after 30 days of immersion at room temperature. It is obvious from Figure 5a that a well-developed copper color, indicating layer dezincification and some pit. After addition of P (Figure 5b), mixed product of corrosion visually, surface was reddened indicating that layer dezincification and shallow occurred, greenish scale (Cu carbonate) and whitish scale (ZnO) cover the surface [46]. A thin layer of light blue scale (presumably malachite) covered the brass surface in the high alkalinity water.

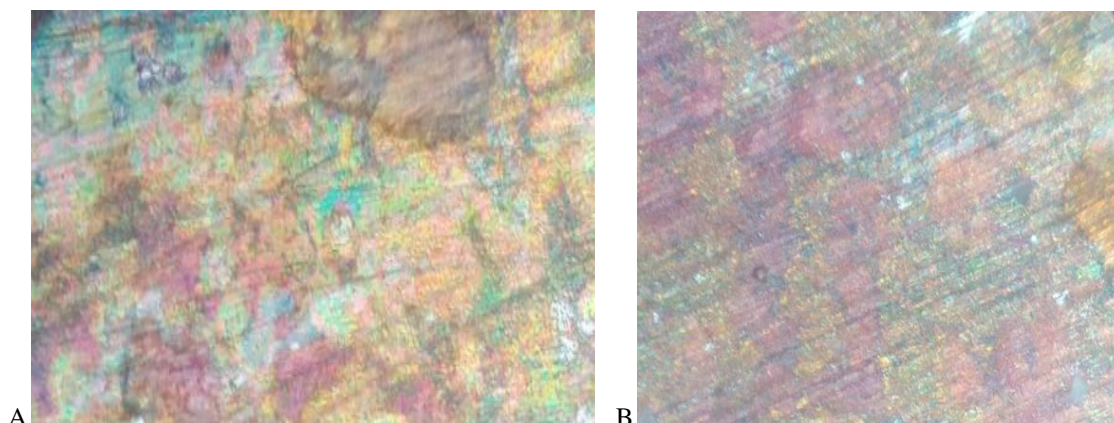


Figure 5: Micrographs of brass surface after 30 days of immersion in SDW-solution: (A) the blank solution and (B) in the presence of 1000 ppm of inhibitor.

4. Conclusion

The inhibition efficiency of mineral product (P) on the corrosion inhibition of brass in simulated drinking water solution have been investigated using EIS, Tafel polarization techniques and optical microscope and the following results obtained:

- ✓ Mineral compound (P) inhibits the corrosion of brass in Simulated Drinking Water (SDW) solution.
- ✓ The inhibition efficiency values increase with increasing inhibitor concentration (P) and showed maximum corrosion inhibition of 84 % at 1000 ppm concentration, above which corrosion rate increases.
- ✓ According to the results, the mineral inhibitor [P] has insignificant effect on corrosion potential and Tafel slopes. Therefore, it is concluded that a cathodic-type inhibitor was behavior predominant.
- ✓ EIS results indicate that as the additive concentration was increased the polarization resistance increased whereas double-layer capacitance decreased.
- ✓ Observation by optical microscopy brass in the middle in the absence and presence of the mineral product (P) shows that the brass studied suffer uniform dezincification in the absence of inhibitor, attenuated effect by the formation of mixed products with inhibitor.

References

1. Jones D.A., Principles and Prevention of Corrosion, 2nd ed.; Prentice-Hall: Upper Saddle River, NJ, 1996.
2. Poling G.W., *Corros. Sci.* 10 (1970) 359.
3. Mansfeld F., Smith T., Parry E.P., *Corrosion* 27 (1971) 289.
4. Gad-Allah A.G., Abou-Romia M.M., Badawy M.W., Rehan H.H., *J. Appl. Electrochem.* 21 (1991) 829.
5. Mitra A.K., R&D J., *NTPC* 2 (1996) 52.
6. Elmorsi M.A., Hassanein A.M., *Corros. Sci.* 41 (1999) 2337.
7. El Bakri M., Touir R., Tazouti A., Dkhireche N., Ebn Touhami M., Rochdi A., Zarrouk A., *Arab. J. Sci. Eng.* 41 (2016) 75.
8. Yohai L., Schreiner W.H., Vázquez M., Valcarce M.B., *J. Solid State Electrochem.* 19 (2015) 1559.
9. Babouri L., Belmokre K., Abdelouas A., Bardeau J.-F., El Mendili, Y., *Int. J. Electrochem. Sci.* 10 (2015) 7818.
10. Jayasree A.C., Ravichandran R., *Int. J. Curr. Microbiol. App. Sci.* 3 (2014) 515.
11. Xavier J.R., Nallaiyan R., *J. Solid State Electrochem.* 16 (2012) 391.
12. Muñoz A.I., Antón J.G., Guiñón J.L., Herranz V.P., *Electrochim. Acta* 50 (2004) 957.
13. Xu Q.J., Zhou G.D., Wang H.F., Cai W.B., *Anti-Corros. Met. Mater.* 53 (2006) 207.
14. Wu X., Chou N., Luper D., Davis L.C., Proceeding of the 13th Annual conference on hazardous, waste research, Snowbird, pp. 374-382, Utah (1998)
15. Okafor P.C., Ikpi M.E., Uwah I.E., Ebenso E.E., Ekpe U.J., Umoren S.A., *Corros. Sci.* 50. (2008) 2310.
16. Obot I.B., Gasem Z.M., Umoren S.A., *Int. J. Electrochem. Sci.* 9 (2014) 510.

17. Matter E.A., Kozhukharov S., Machkova M., Kozhukharov V., *Mater. Corros.* 64 (2013) 408.
18. Miao S.T., Han S., Hao L., *Adv. Mater. Research* 881-883 (2014) 1165.
19. Aramaki K., *Corros. Sci.* 43 (2001) 1573.
20. Singh R.N., Tiwari S.K., Singh W.R., *J. Alloys Compd.* 22 (1992) 1175.
21. Nam N.D., Mathesh M., Hinton B., Tan M.J.Y., Forsyth M., *J. Electrochem. Soc.* 161 (2014) C527.
22. Aramaki K., *Corros. Sci.* 49 (2007) 1963.
23. Lin S., Fang S.K., *J. Electrochem. Soc.* 152 (2005) B54.
24. Xiong R. C., Zhou Q., Wei G., *Chin. Chem. Lett.* 14 (2003) 955.
25. Sarver E., Edwards M., *Corros. Sci.* 53 (2011) 1813.
26. Valcarce M.B., Vázquez M., *Corros. Sci.* 2 (2010) 1413.
27. Yohai L., Vázquez M., Valcarce M. B., *Corros. Sci.* 53 (2011) 1130.
28. McCafferty E., *Corros. Sci.* 47 (2005) 3202.
29. Gao G., Liang C., *Electrochim.* 52 (2007) 4554.
30. Oguzie E.E., Li Y., Wang F.H., *J. Colloid Interf. Sci.* 310 (2007) 90.
31. El-Hajjaji F., Belkhmira R.A., Zerga B., Sfaira M., Taleb M., Ebn Touhami M., Hammouti B., *J. Mater. Environ. Sci.* 5 (2014) 263-270
32. Ramde T., Rossi S., Zanella C., *Appl. Surf. Sci.* 307 (2014) 209.
33. Keles H., *Mater. Chem. Phys.* 130 (2011) 1317.
34. Deng S., Li X., Fu H., *Corros. Sci.* 53 (2011) 3596.
35. Keles H., Solmaz R., Özcan M., Kardas G., Dehri I., *Surf.Coat. Tech.* 203 (2009) 1469.
36. Solmaz R., *Corros. Sci.* 52 (2010) 3321.
37. Conway B.E., Impedance behavior of electrochemical supercapacitors and porous electrodes, in: Barsoukov E., Macdonald J.R. (Eds.), *Impedance Spectroscopy Theory, Experiment, and Applications*, John Wiley and Sons Inc., New Jersey, 2005, pp. 494-497.
38. Halim A., Watkin E., Gubner R., *Electrochim. Acta* 77 (2012) 348.
39. Ashassi-Sorkhabi H., Asghari E., *J. Appl. Electrochem.* 40 (2010) 631.
40. Negm N.A., Zaki M.F., Said M.M., Morsy, S.M., *Corros. Sci.* 53 (2011) 4233.
41. Fengling X., Jizhou D., Shufang Z., Baorong H., *Mater. Lett.* 62 (2008) 4072.
42. Erbil M., *Korozyon: İlkeler ve Önlemler*. The Corrosion Association Publication, Ankara, Turkey (2012).
43. Raj X.J., Rajendran N., *Int. J. Electrochem. Sci.* 6 (2011) 348.
44. Moretti G., Guidi F., Fabris F., *Corros. Sci.* 76 (2013) 206.
45. Umoren S.A., Solomon M.M., Eduok U.M., Obot I.B., Israel A.U., *J. Environ. Chem. Eng.* 2 (2014) 1048.
46. Maynard B., Mast D., Boyd G., «Kinetics of Lead Release From Brass Water Meters and Faucets», *Proc 2008 AWWA WQTC Cincinnati*, (2008).

(2016) ; <http://www.jmaterenvironsci.com/>